Dyes and Pigments 103 (2014) 161–167

Contents lists available at ScienceDirect

Dyes and Pigments

journal homepage: www.elsevier.com/locate/dyepig

Molecular design for the highly-sensitive piezochromic fluorophores with tri-armed framework containing triphenyl-quinoline moiety

Tai-Shen Hsiao, Tai-Lin Chen, Wei-Lun Chien, Jin-Long Hong*

Department of Materials and Optoelectronic Science, National Sun Yat-Sen University, Kaohsiung 80424, Taiwan

ARTICLE INFO

Article history:
Received 13 September 2013
Received in revised form
13 November 2013
Accepted 14 November 2013
Available online 2 December 2013

Keywords:
Piezochromic fluorescence
Solvatochromism
Tri-arm
Bathochromic shift
Planarization
Triphenylamino-quinoline

ABSTRACT

Two tri-armed piezochromic fluorescent molecules of tris(4-(4-phenylquinolin-2-yl)phenyl)amine (TPA-3Qu) and tris(4-(6-(9*H*-carbazol-9-yl)-4-phenylquinolin-2-yl)phenyl)amine (TPA-3QuCz) were prepared and found to exhibit keen fluorescence responses toward compression. With the framework of a twisted, pyramidal triphenylamine (TPA) center connecting to three large quinolinecarbazole (QuCz) arms, the amorphous TPA-3QuCz exhibited a large bathochromic shift of 112 nm under gentle grinding forces, which is different from the small shift of 32 nm for TPA-3Qu under applying a relatively-large pressure of 10 MPa. Conformational transformations involving planarization of the arms were proposed to account for the observed fluorescence responses of TPA-3QuCz and TPA-3Qu towards pressure.

1. Introduction

Organic fluorophores exhibiting color and fluorescence changes upon external pressure stimuli have drawn lots of attention due to their convenient tunability and high sensitivity. These piezochromic fluorescent materials have promising practical applications [1], such as mechano-sensors, security papers, data storage, and also opto-electronic devices. Most mechanisms responsible for the piezochromic fluorescence involved the changes of intermolecular stacking under external pressure stimulus [2–29]. For example, the intermolecular transformation process involved in the compression of the cyanodistyrylbenzene derivative [13] caused the corresponding fluorescent color change from blue (B-phase) to green (G-phase) due to two distinctive crystal packings with varied π–π overlap. Despite the prevalent intermolecular transformation mechanism, the piezochromism of a donor–acceptor anthraquinone imide [28] system was nevertheless due to an intramolecular process, in which the single-bond linking donor and acceptor groups rotates to result in molecular planarization and therefore, the alternation on the fluorescent color. New piezochromic fluorophores with different structural frameworks are still in demand and in view that new architecture provides access for the real conformational transformation responsible for the piezofluorochromism.

To have an efficient fluorescence recording system, piezochromic fluorescent materials need to have full coverage of wide emissive color spectrum under small load of pressure stimuli. Most of the conventional systems illustrated a relatively-small bathochromic shift (<50 nm) under pressure stimuli. Until now, the largest emission shift is 124 nm (from green (528 nm) to red (652 nm)) observed for bis((pyrid-2-yl)vinyl)anthracene [16]; however, such drastic fluorescence change was achieved by a large pressure load of 8 GPa. Under compression, the crystalline stacking between adjacent anthracene rings transformed into a more compact arrangement to result in the observed fluorescence red-shift.

Piezofluorochromism refers to the pressure-induced shortening of the intermolecular distance and the cocurrent electronic orbital overlap to result in the observed bathochromic shift. To maximize electronic orbital overlap, most piezochromic fluorescent molecules have the architecture with a large planar center connected by rotable substituents, which undergo geometrical adjustment to result in a conformer with different fluorescent wavelengths. Instead of the normal planar central ring, piezofluorochromic TPA-3Qu and TPA-3QuCz (Scheme 1) investigated in this study possess a highly-twisted pyramidal triphenylamine (PA) center, to which two different quinoline arms (Qu and QuCz, respectively) were linked to

* Corresponding author.
E-mail addresses: joe79727@gmail.com (T.-S. Hsiao), solar77411@hotmail.com (T.-L. Chen), jacky0149@gmail.com (W.-L. Chien), jlhong@mail.nsysu.edu.tw (J.-L. Hong).

0143-7208/$ – see front matter © 2013 Elsevier Ltd. All rights reserved.
http://dx.doi.org/10.1016/j.dyepig.2013.11.016

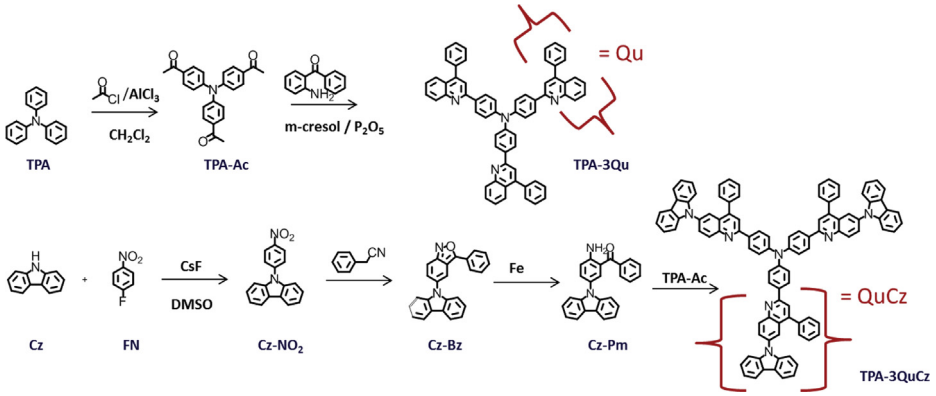

Scheme 1. Syntheses of TPA-3Qu and TPA-3QuCz.

induce distinct fluorescence responses. Comparatively, TPA-3Qu with relatively-smaller Qu arms is crystalline material exhibiting smaller fluorescence shift of 32 nm after a pressure load of 10 MPa. The varied sensitivity in relationship to the arm structure of TPA-3QuCz and TPA-3Qu and the pressure-induced structural transformation of the arms are therefore the main focus of this study.

2. Experimental section

2.1. Instrumentations and sample preparations

The wide-angle X-ray diffraction (WAXD) was obtained with a Siemen D5000 X-ray diffractometer with a source of CuK radiations at 40 kV and 30 mA. Diffractions patterns were collected with a scan rate of 0.1°/3 s from the 2θ ranges of 2–60°. A mass spectrum was obtained by using a BrukerDaltonicsAutoflex III MALDI-TOF mass spectrometer. Photo luminescence (PL) spectra were obtained from a LabGuide X350 FL spectrophotometer using a 450 W Xe lamp as the continuous light source. ^{1}H NMR spectra were recorded with a VarianVXR-500 MHz FT-NMR instrument which use tetramethylsilane (TMS; $\delta = 0$ ppm) as internal standard. The UV–vis absorption spectra were recorded with an Ocean Optics DT 1000 CE 376 spectrophotometer. Elemental analyses were performed on an Elementary Vario EL-III C, H, and N analyzer. Melting point (T_m) of organic compound and glass transition temperature (T_g) of oligomer were determined from a TA Q-20 differential scanning calorimeter (DSC) with a scan rate of 10 °C/min under nitrogen. All solid samples were sealed in a hermetic pan before DSC scan.

The initial samples were placed in a mortar and were gently ground by pestle to obtain the ground samples. Powers in an IR demountable cell holder were also pressurized by a hydraulic presser to obtain pressurized pellets by desired pressure load. The sample powders were primarily heated in hotplate to the desired temperatures before immediate withdrawal to obtain air-quenched powder as the heated samples for analysis. All compressed samples were subjected to solvent annealing by placing them in a closed chamber saturated with triethylamine (TEA) vapor for 10 h to result in the solvent-annealed samples. Pellets after different treatments were then investigated by fluorescence spectrometer, WAXD and DSC.

2.2. Synthesis

Triphenylamine (TPA), 2-aminobenzophenone, aluminum chloride, acetyl chloride, acetic acid, phosphorus pentoxide (P_2O_5), carbazole (Cz), 1-fluoro-4-nitrobenzene (FN) and benzyl cyanide were purchased from Aldrich Chemical Co. and used directly without further purification. THF was refluxed over sodium and benzophenone under nitrogen for more than 2 days before distillation for use. Triethylamine, dichloromethane and *m*-cresol were distilled from CaH_2 under nitrogen before use.

2.2.1. Synthesis of TPA-3QuCz and TPA-3Qu

TPA-3Qu and TPA-3QuCz compounds were prepared according to the procedures illustrated in the Scheme 1 and details are given below.

2.2.2. 1,1′,1″-(Nitrilotris(benzene-4,1-diyl)) triethanone (TPA-Ac)

Triphenylamine (1 g, 4.08 mmol), anhydrous DCM (20 mL) and $AlCl_3$ (1.69 g, 12.64 mmol) were added to a three-neck flask under nitrogen atmosphere and the whole mixtures were cooled to 0 °C by ice-water bath. Acetyl chloride (1 g, 12.64 mmol) was then added dropwise to the stirred reaction mixture at 0 °C. The reaction was allowed to warm to room temperature and continued for overnight. The resulting mixture was poured into ice water (125 mL), and the organic layer was collected, concentrated, and poured into a large amount of ethanol. The yellow green precipitates were collected and purified by column chromatography (EtOAc/hexane $v/v = 1/9$) to give TPA-Ac (1.45 g, yield 95%). Mp: 160 °C; ^{1}H NMR (500 MHz, $CDCl_3$): δ 2.55 (9H, s), 7.16 (6H, d, $J = 8.5$ Hz), 7.9 (6H, d, $J = 6$ Hz); *m*/*z* (EI MS) Calcd for $C_{24}H_{21}NO_3$, 371.15; Found, 371.11; Anal. Calcd for $C_{24}H_{21}NO_3$: C, 77.61; H, 5.70; N, 3.77. Found: C, 77.34; H, 5.81; N, 3.10.

2.2.3. N-(4-Nitrophenyl)carbazole (Cz-NO$_2$)

To the stirred solution mixtures of carbazole (2 g; 10 mmol) and of 4-fluoronitrobenzene (2.11 g; 15 mmol) in dried DMSO (10 mL), dried cesium fluoride (3.04 g; 20 mmol) was added at once, and the mixtures were heated at 150 °C for 15 h under nitrogen atmosphere. The resultant products were slowly added into stirred methanol (60 mL). The precipitated yellow crystals were collected by filtration and washed thoroughly with methanol. After filtration, yellow Cz-NO_2 crystal (2.82 g; yield 98%) was obtained. Mp: 210 °C; ^{1}H NMR (500 MHz, $CDCl_3$): δ 7.33 (3H, t, $J = 7$ Hz), 7.45 (3H, td, $J = 6$, 1 Hz), 7.55 (2H, d, $J = 7.8$ Hz), 7.96 (2H, dt, $J = 13.5$, 3.5 Hz), 8.26 (2H, d, $J = 7.5$ Hz), 8.49 (2H, dt, $J = 9$, 2.5 Hz); *m*/*z* (EI MS) Calcd for $C_{18}H_{12}N_2O_2$, 288.30; Found 288.35. Anal. Calcd for $C_{18}H_{12}N_2O_2$:C, 74.99; H, 4.20; N, 9.72. Found: C, 74.96; H, 4.27; N, 9.85.

2.2.4. 5-(9H-carbazol-9-yl)-3-phenylbenzo[c]isoxazole (Cz-Bz)

To an ice-cooled mixture of sodium hydroxide (4.68 g, 117 mmol), methanol (30 mL), and THF (50 mL), benzyl nitrile (1.27 g, 10.8 mmol) was added slowly. After stirring for 1 h, Cz-NO_2 (2.82 g, 9.78 mmol) was added and the whole mixtures were then

heated at 80 °C for 20 h. The products were then cooled in an ice-water bath and the precipitate was filtered and exhaustively washed with cold methanol. The crude product was purified by column chromatography (CH_2Cl_2) to give Cz-Bz (1.41 g; 40%). Mp: 221 °C; ^{1}H NMR (500 MHz, $CDCl_3$): δ 7.26–7.35 (2H, tt, J = 14, 7 Hz), 7.85–7.87 (1H, d, J = 9 Hz), 8.01–8.03 (2H, d, J = 5 Hz), 8.06 (1H, s), 8.17–8.18 (2H, d, J = 7.5 Hz); m/z (EI MS): Calcd for $C_{25}H_{16}N_2O$, 360.13; Found, 360.25; Anal. Calcd for $C_{25}H_{16}N_2O$: C, 83.31; H, 4.47; N, 7.77. Found: C, 83.35; H, 4.54; N, 7.63.

2.2.5. (2-Amino-5-(9H-carbazol-9-yl)phenyl)(phenyl)methanone (Cz-Pm)

Iron powder (4 g, 71.63 mmol) and water (4 mL) were added to a stirred suspension of Cz-Bz (1.41 g, 3.91 mmol) in acetic acid (100 mL). The reaction mixtures were then heated at 95 °C for 24 h before cooled to room temperature to remove the iron powder by filtration. The filtrates were then poured into water (500 mL) and the filtered precipitate was collected and purified by column chromatography (EtOAc/hexane: v/v = 1/5) to give Cz-Pm (1.27 g, 90%). Mp: 258 °C; ^{1}H NMR (500 MHz, $CDCl_3$): δ 7.14–7.52 (12H, m), 7.64 (1H, s), 7.79–7.85 (1H, t, J = 15 Hz), 8.17–8.22 (2H, dd, J = 24, 4.5 Hz), 10.26 (2H, s); m/z (EI MS): Calcd for $C_{25}H_{18}N_2O$, 362.14; Found, 362.10; Anal. Calcd for $C_{25}H_{18}N_2O$: C, 82.85; H,5.01; N, 7.73. Found: C, 82.82; H, 5.10; N, 7.66.

2.2.6. Tris(4-(6-(9H-carbazol-9-yl)-4-phenylquinolin-2-yl)phenyl) amine (TPA-3QuCz)

A solution of P_2O_5 (5 g, 20 mmol) in m-cresol (5 mL) was heated at 135 °C for 2 h. After cooling to room temperatures, Cz-Pm (1.27 g, 3.5 mmol) and TPA-Ac (0.43 g, 1.17 mmol) were added and the whole mixture was heated at 135 °C for another 12 h. After cooled to room temperature, the products were precipitated from a triethylamine/ethanol (v/v = 1/9; 150 mL) solution to give TPA-3QuCz (0.93 g, yield 60%). T_g: 200 °C; FT-IR (KBr, cm^{-1}): 748, 836, 1178, 1228, 1282, 1314, 1330, 1360, 1394, 1448, 1492, 1510, 1542, 1588, 1620, 2351, 2852, 2924, 2952, 3043; ^{1}H NMR (500 MHz, $CDCl_3$): δ 7.30–7.33 (6H, t, J = 5 Hz), 7.39–7.41 (6H, d, J = 10 Hz), 7.44–7.71 (21H, m), 7.75–7.76 (6H, d, J = 20 Hz), 7.94 (3H, d, J = 20 Hz), 8.08–8.1(3H, d, J = 10 Hz), 8.19 (6H, s), 8.25–8.26 (6H, d, J = 5 Hz), 8.43–8.45 (3H, d, J = 10 Hz), 8.46–8.48 (3H, d, J = 10 Hz); m/z (EI MS): Calcd for $C_{99}H_{63}N_7$, 1350.52; Found, 1350.50. Anal. Calcd for $C_{99}H_{63}N_7$: C, 88.04 H, 4.7 N, 7.26. Found: C, 87.84, N, 4.81, H, 7.35.

2.2.7. Tris(4-(4-phenylquinolin-2-yl)phenyl)amine (TPA-3Qu)

A solution of P_2O_5 (15 g, 59.95 mmol) in m-cresol (15 mL) was heated at 135 °C for 2 h. After cooling to room temperatures, 2-aminobenzophenone (2.31 g, 11.7 mmol) and TPA-Ac (1.45 g, 3.9 mmol) were added. The whole mixture was heated to 135 °C for another 12 h. The products after cooling were then precipitated from a triethylamine/ethanol (v/v = 10/90; 150 mL) solution to give TPA-3Qu (2 g, yield 60%). Mp: 208 °C; FT-IR (KBr, cm^{-1}): 701, 770, 840, 1151, 1177, 1237, 1285, 1319, 1357, 1455, 1488, 1509, 1539, 1590, 3030, 3055; ^{1}H NMR (500 MHz, $CDCl_3$): δ 7.34-7.36 (6H, d, J = 8.5 Hz), 7.45–7.59 (18H, m), 7.71–7.74 (3H, t, J = 9 Hz), 7.8 (3H, s), 7.89–7.9 (3H, d, J = 4.5 Hz), 8.12–8.14 (6H, d, J = 8.5 Hz), 8.22–8.24 (3H, d, J = 5 Hz); MS m/z: Calcd for $C_{63}H_{42}N_4$, 854.34; Found, 854.24 (M^+). Anal. Calcd for $C_{63}H_{42}N_4$:C, 88.50; H, 4.95; N, 6.55. Found: C, 88.45 H, 4.90; N, 6.65.

3. Results and discussion

3.1. Synthesis and characterization

The target compounds TPA-3QuCz and TPA-3Qu were synthesized according to Scheme 1, in which Friedländer condensation between an o-amino ketone and acetyl group is the main reaction to construct the desired quinoline rings in TPA-3Qu and TPA-3QuCz. Primarily, the key intermediate TPA-Ac was prepared from the simple Friedel–Crafts acetylation of TPA in the presence of acetyl chloride/$AlCl_3$. Friedländer condensation between TPA and o-aminobenzophene (AB) afforded the first target compound of TPA-Ac. For the preparation of another target compound TPA-3QuCz, the key intermediate Cz-Pm containing o-amino ketone needs to be synthesized by a three-step reaction procedure. The most versatile and useful method for synthesizing o-amino ketones was a route via the generation of benzisoxazole from an aromatic nitro compound, followed by reductive cleavage of the benzisoxazole. Accordingly, Cz-NO_2 with one nitro group was synthesized by the nucleophilic addition of carbazole to 1-fluoro-4-nitrobenzene (FN). The resultant Cz-NO_2 was then subjected to the Stille process, in which Cz-NO_2 was further reacted with benzyl nitrile to generate CzBz with benzisoxazole ring, followed by the reduction with iron to obtain the desired Cz-Pm. Friedländer condensation between Cz-Pm and TPA-Ac resulted in the second target compound of TPA-3QuCz. The molecular structures of all intermediates and final products were confirmed by ^{1}H NMR spectroscopy, mass spectrometry and elemental analysis.

3.2. TPA-3QuCz and TPA-3Qu solid-state fluorescence behavior

All fluorescence responses of TPA-3QuCz and TPA-3Qu towards pressure and solvent-fuming processes were illustrated in Fig. 1. Grinding the TPA-3QuCz powder in a mortar readily changed its fluorescence color from green to orange and higher pressure load (10 MPa) by pressing TPA-3QuCz in a hydraulic presser further switched the fluorescence color to red. Grinding and high-pressure loading also caused the changes of sample colors from yellow to pale brown and then from pale brown to orange, respectively. The pressed TPA-3QuCz can be reversed back to the pristine state (yellow color and green fluorescence) by fuming the sample in a close chamber saturated with triethylamine (TEA) vapor. In contrast to the highly-sensitive TPA-3QuCz, grinding caused no change on the crystalline TPA-3Qu and a higher pressure load of 10 MPa was required to produce noticeable changes on the color (from yellow to brown) and the fluorescence (from yellow to orange). The pressed TPA-3Qu can be also reversed to the initial state by TEA-fuming. The above-mentioned color and fluorescence changes are so significant that one can easily distinguish them by direct observation.

The spectral responses towards compression were then monitored. As illustrated in Fig. 2A, the PL emission spectrum of the initial TPA-3QuCz showed only one broad band located at 500 nm and grinding caused the emergence of a new band at 612 nm. High-pressure (10 MPa) loading completely transformed all emission bands into a new one located at a longer wavelength of 627 nm and the resultant emission intensity is actually larger than the initial and the ground samples. Subsequent TEA-fuming transformed the pressed TPA-3QuCz into the pristine state in view that the TEA-fumed sample emitted similarly with the initial sample. For TPA-3Qu, a high-pressure load of 10 MPa was required to cause a small bathochromic shift of 32 nm (Fig. 2B) in the emission spectra and TEA-fuming also successfully transformed the pressed sample to the original one as evidenced by the corresponding emission spectra. For TPA-3QuCz and TPA-3Qu, the wavelength changes caused by compression/TEA-fuming cycle can be repeated several times without noticeable fatigue, which suggests the excellent reversibility of both samples.

To clarify the possible molecular transformation modes during compression, wide-angle X-ray diffraction (WAXD) analysis was conducted. As expected, the initial TPA-3QuCz powders are

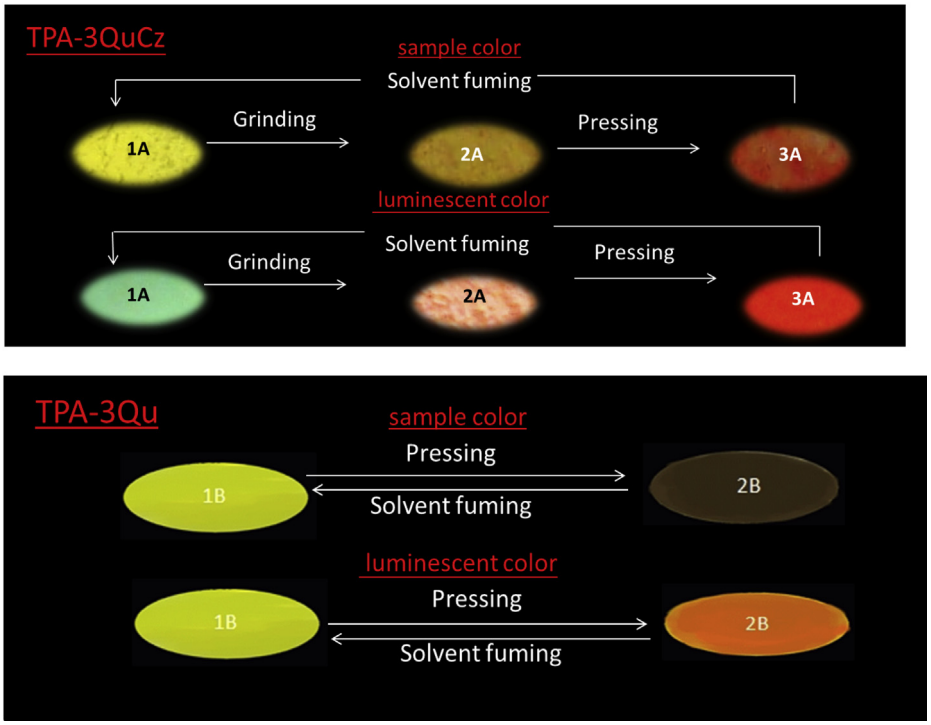

Fig. 1. Color (top) and fluorescence (bottom) changes of TPA-3QuCz powders (1A–3A) and TPA-3QuCz powders (1B–2B) upon compression and TEA-fuming processes (fluorescence was observed by irradiated with a 365-nm UV light).

amorphous materials with no sharp, crystalline (Fig. 3A) diffraction peak; instead, the overlapped broad bands in the low- (corresponding to *d* spacing in the ranges of 2.4–8.8 Å) and high- (1.8–4.0 Å) angle regions suggest the presence of two macroscopic intermolecular distances in the tri-armed TPA-3QuCz. The sensitivity of the tri-arm structure towards pressure change can be verified by the fact that gentle grinding completely demolished the structure representing the high-angle diffraction peak. After high-pressure load (10 MPa), the low-angle diffraction band however survived and remained intact, which indicates that no more macroscopic structural changes occurred during further compression. Again, the recovery of the two-band pattern in the TEA-fumed sample represents the regeneration of the original state by TEA-fuming of the pressurized TPA-3QuCz.

The sharp diffraction peaks in Fig. 3B suggest that the TPA-3Qu powder is a crystalline material. The sharp diffraction peaks were mostly destroyed after compression and the remaining tiny peaks refer to the amorphous nature of the pressed sample. The varied molecular stacking modes between the crystalline and the amorphous metastable samples are therefore responsible for the observed piezofluorochromism of TPA-3Qu. TEA-fuming recovered the crystalline structure as evidenced by the regenerated sharp diffraction peaks.

Pressure-induced structure changes can be monitored by DSC. The initial TPA-3QuCz (Fig. 4A) exhibited a broad glass transition (T_g) extended from 180 to 215 °C, which is different from the narrow transition (from 212 to 220 °C) observed for the ground sample of TPA-3QuCz. The broad and the narrow transition features are consistent with the double and the single WAXD peaks (Fig. 3A) resolved in the initial and in the ground TPA-3QuCz, respectively. Continuous compression raised T_g to a higher level of 222–232 °C. Increase of T_g indicates that compression transformed TPA-3QuCz into a structure that was difficulty to agitate by thermal energy. Again, TEA-fuming recovered the structure as viewed by the regenerated broad transition feature.

DSC thermograms in Fig. 4B suggest that the initial TPA-3Qu is crystalline material with the detected T_m at around 208 °C. Subsequent compression caused no major change on the DSC thermogram but the presence of a tiny melting–recrystallization peak at 107 °C (inset) suggests the presence of new metastable phase in

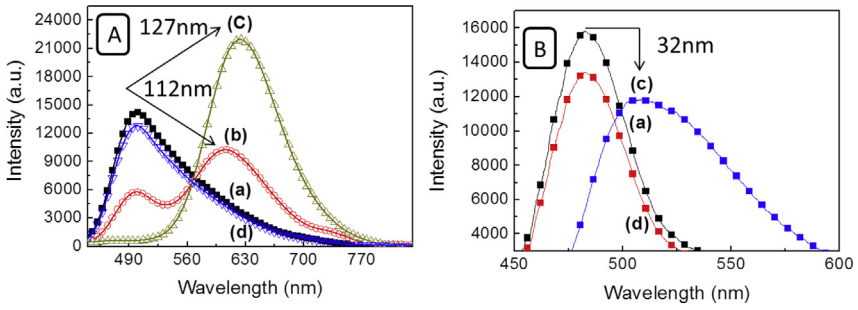

Fig. 2. Emission spectra of (A) TPA-3QuCz and (B) TPA-3Qu for (a) the initial samples and sample after b) grinding, c) compression and d) TEA-fuming (λ_{ex} = 390 nm).

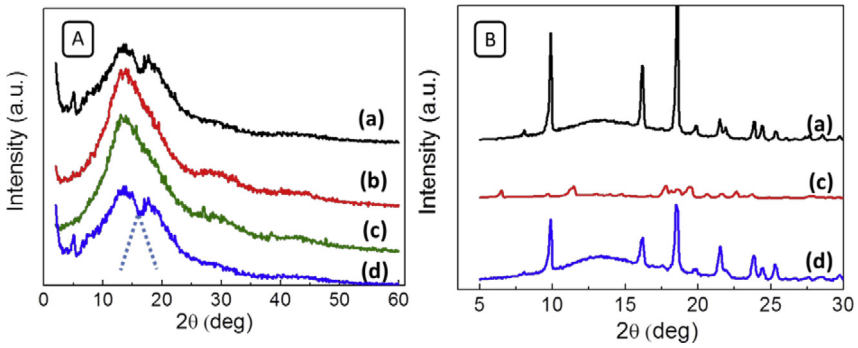

Fig. 3. The WAXD spectra of (A) TPA-3QuCz and (B)TPA-3Qu for (a) the initial samples and sample after b) grinding, c) compression and d) TEA-fuming.

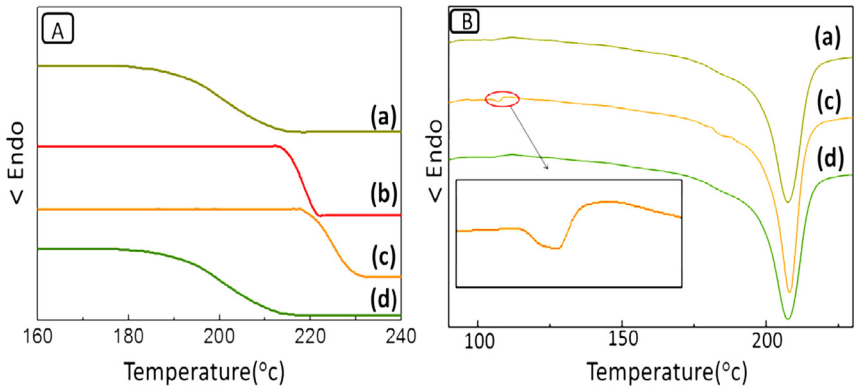

Fig. 4. DSC thermograms of (A) TPA-3QuCz and (B) TPA-3Qu for (a) the initial samples and sample after b) grinding, c) compression and d) TEA-fuming. (heating rate = 10 °C/min).

the pressed sample. The DSC thermogram of the pressed TPA-3Qu is similar to that reported for the piezofluorochromic phenothiazine–anthracene materials [23]; therefore, same transformation mechanism that melt state of the pressed TPA-3Qu would transfer to a more stable state, corresponding to the main melting transition at 208 °C, through multiple melt-recrystallization process during DSC scan before final melting, was proposed here. After solvent-fuming, the tiny melting-recrystallization peak at 107 °C disappeared and the corresponding DSC thermogram is essentially identical with the initial one.

The complicated pressure-induced conformation transformation of TPA-3QuCz can be best evaluated from the model TPA-3Qu in view of their structural similarity and fortunately, a single crystal of TPA-3Qu can be grown from methylene chloride/hexane solvent pair and therefore its crystalline structure can be determined from the single-crystal X-ray diffraction analysis. The resultant single-molecule conformer (Fig. 5) adopts a twisted tri-arm framework with a dihedral angle of 145.6° in between the two bonds jointing the Qu arm and the central nitrogen atom of the TPA center. In each of the Qu arms, the phenylene (A ring) and the quinoline (B ring) units are nearly parallel to each other and constitute a rigid confacial plane perpendicular to the 3-phenyl (C ring) substituent of the quinoline unit. The intermolecular hydrogen-bond (H-bond) interaction between quinoline N-atom and the benzene *para*-C-H of the 3-phenyl (C ring) substituent form the closest intermolecular distance of 1.78 Å.

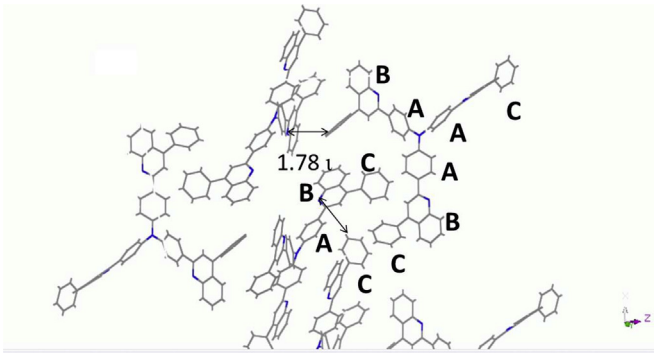

Fig. 5. The crystal lattice of TPA-3Qu determined from single-crystal X-ray diffraction analysis.

The twisted, pyramidal TPA center of TPA-3Qu created large amounts of defects existing in the interfacial area and the imperfect crystal lattices can be destroyed through slip deformation triggered by external pressure. Because the perpendicular C ring is the closest unit neighboring to the quinoline N-atom of another molecule and conceptually, it will be the most probable one subjected to conformational change under pressure. During the intial slip deformation course, two neighboring TPA-3Qu molecules (Scheme 2) will pass through each other and the intermolecular steric repulsions forced the neighboring, perpendicular C rings to rotate to a position more co-facial to the rest of the Qu arm (mainly, A and B rings), leading to the breakage of the weak H-bonds and the formation of planarized arms with long conjugation to account for the observed bathochromic shift during compression. The proposed transformation is basically similar to the piezofluorochromic compound containing a phenothiazine and an anthracene moieties [23].

To probe for possible structural transformation for the amorphous TPA-3QuCz, molecular computation using Molecular Studio (*MS*) software was conducted. The minimum-energy, single-molecule conformer in Scheme 3 (upper) also possesses a highly-

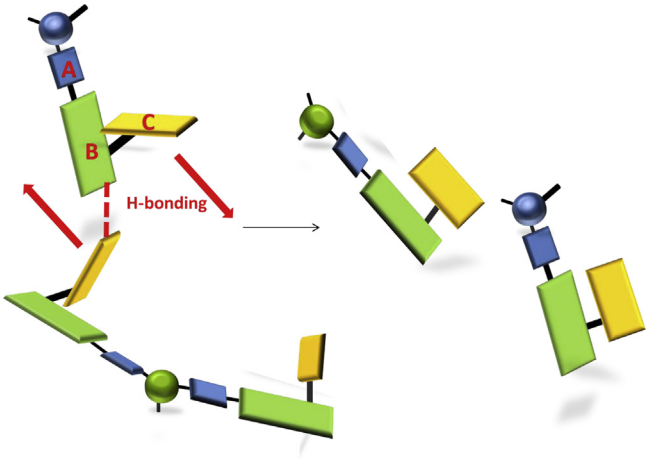

Scheme 2. The planarization of Qu arms during compression of TPA-3Qu.

twisted pyramidal TPA center. Most notable feature of the resultant conformer is that the terminal carbazole and 3-phenyl (C ring) rings of the QuCz arms are arrayed nearly perpendicular to the rigid plane constituted by the co-facial A and B rings (lower Scheme 3). Here, the bulky carbazole termini create interfacial defects resulting in the observed amorphous disorder. During the slip deformation trigged by grinding forces, the large carbazole rings were the initial points subjected to conformational transformation and will rotate to a position more paralleling to the co-facial A and B rings, leading to extended conjugation correlated to the observed large bathochromic shift of 112 nm. Before grinding, the intermolecular

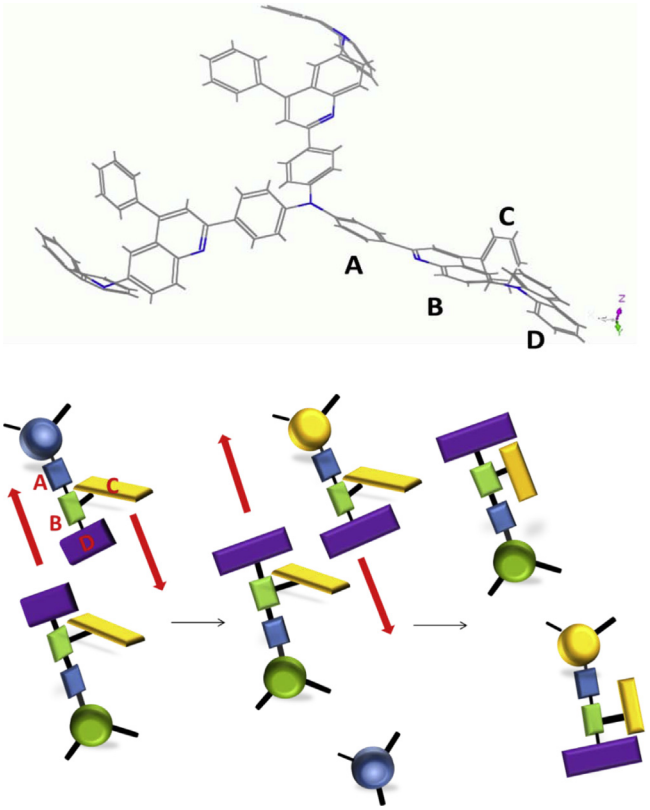

Scheme 3. The energy-minimized conformer (upper) of TPA-3QuCz simulated from Molecular studio (MS) software and the planarization (lower) of QuCz arm during compression of TPA-3QuCz.

distances between perpendicular carbazole rings and the neighboring molecules are responsible for the broad WXRD diffractions in the high-angle regions (cf. Fig. 3A); after grinding, planarization of the carbazole ring resulted in the disappearance of the structure units with small intermolecular distances and only structural units with longer intermolecular distances survived. After grinding, TPA-3QuCz molecules with planarized arms generate amorphous structures with less interfacial defects, which may be responsible for the observed high T_g (cf. Fig. 4A) of the ground sample of TPA-3QuCz.

Further compression resulted in no macroscopic structural change as judged by the immobile WAXD spectra (Fig. 3A); nevertheless, certain conformational change must occur in order to correlate with the observed bathochromic shift of the fluorescence spectrum (cf. Fig. 2A). The intact WAXD spectra before and after compression may only indicate that there was no further macroscopic conformational change but instead a minor change involving small adjustment on the perpendicular 3-phenyl ring (C ring) may be responsible for the continued bathochromic shift (~15 nm) at this stage. Similarly, C rings rotated to a position more paralleling to the rest of the rigid portions in the already-planarized arm, resulting in the extension of the conjugation length and the observed bathochromic shift.

4. Conclusion

In summary, a highly-sensitive piezofluorochromic amorphous material of TPA-3QuCz was prepared and was shown to have a large bathochromic shift of 112 and 127 nm after grinding and pressing, respectively; in contrast, crystalline TPA-3Qu with small arms showed a comparatively smaller shift of 32 nm after compression. Molecular transformation mechanism with continuous planarization of the arms was proposed to account for the observed piezofluorochromism. Slip deformation caused the rotation of the perpendicular carbazole (or 3-phenyl) ring to a position more cofacial to the rest of the arm units, leading to the extended conjugation lengths and the observed bathochromic shifts in both TPA-3QuCz and TPA-3Qu systems.

Acknowledgments

We appreciate the financial support from National Science Council, Taiwan, R.O.C. under the projects No. 102-2221-E-110-084-MY3 and 102-2221-E-110-080.

Appendix A. Supplementary data

Supplementary data related to this article can be found at http://dx.doi.org/10.1016/j.dyepig.2013.11.016.

References

[1] Yerushalmi R, Scherz A, Boom ME, Kraatz HB. Stimuli responsive materials: new avenues toward smart organic devices. J Mater Chem 2005;15:4480–7.
[2] Gawinecki R, Dobosz R, Zakrzewska A. Effect of the amino group on the property of 1-(benzylideneamino)pyridinium salts. Dye Pigment 2004;60:143–5.
[3] Gawinecki R, Viscardi G, Barni E, Hanna MA. 4-Tert-butyl-1-(4′-dimethylamino-benzylideneamino)pyridinium perchlorate (BDPP) – a novel fluorescent dye 1993;23:73–8.
[4] Pucci A, Ruggeri G. Mechanochromic polymer blends. J Mater Chem 2011;21:8282–91.
[5] Ariga K, Mori T, Hill JP. Mechanical controls of nanomaterials and nanosystems. Adv Mater 2012;24:158–76.
[6] Lowe C, Weder C. Oligo(p-phenylene vinylene) excimers as molecular probes: deformation-induced color changes in photoluminescent polymer blends. Adv Mater 2002;14:1625–9.

[7] Kunzelman J, Kinami M, Crenshaw BR, Protasiewicz JD, Weder C. Oligo(p-phenylene vinylene)s as a "new" class of piezochromic fluorophores. Adv Mater 2008;20:119–22.
[8] Mizoshita N, Tani T, Inagaki S. Isothermally reversible fluorescence switching of a mechanochromic perylene bisimide dye. Adv Mater 2012;24:3350–5.
[9] Kwon MS, Gierschner J, Yoon SJ, Park SY. Unique piezochromic fluorescence behavior of dicyanodistyrylbenzene based donor–acceptor–donor triad: mechanically controlled photo-induced electron transfer (eT) in molecular assemblies. Adv Mater 2012;24:5487–92.
[10] Luo X, Li J, Li C, Heng L, Dong YQ, Bo ZZ, et al. Reversible switching of the emission of diphenyldibenzofulvenes by thermal and mechanical stimuli. Adv Mater 2011;23:3261–5.
[11] Sagara Y, Mutai T, Yoshikawa I, Araki IK. Material design for piezochromic luminescence: hydrogen-bond-directed assemblies of a pyrene derivative. J Am Chem Soc 2007;129:1520–1.
[12] Zhang G, Lu J, Sabat M, Fraser CL. Polymorphism and reversible mechanochromic luminescence for solid-state difluoroboron azobenzene. J Am Chem Soc 2010;13:2160–2.
[13] Yoon SJ, Chung JW, Gierschner J, Kim KS, Choi MG, Kim D, et al. Multistimuli two-color luminescence switching via different slip-stacking of highly fluorescent molecular sheet. J Am Chem Soc 2010;132:13675–83.
[14] Wang J, Mei J, Hu R, Sun JZ, Tang BZ. Click synthesis, aggregation-induced emission, E/Z isomerization, self-organization, and multiple chromisms of pure stereoisomers of a tetraphenylethene-cored luminogen. J Am Chem Soc 2012;134:9956–66.
[15] Teng MJ, Jia XR, Chen XF, Wei Y. A dipeptide-based multicolored-switching luminescent solid material: when molecular assemblies meet mechanochemical reaction. Angew Chem Int Ed Engl 2012;51:6398–401.
[16] Dong Y, Xu B, Zhang J, Tan X, Wang L, Chen J, et al. Piezochromic luminescence based on the molecular aggregation of 9,10-bis((E)-2-(pyrid-2-yl)vinyl) anthracene. Angew Chem Int Ed Engl 2012;51:10782–5.
[17] Dou C, Han L, Zhao S, Zhang H, Wang Y. Multi-stimuli-responsive fluorescence switching of a donor–acceptor π-conjugated compound. J Phys Chem Lett 2011;2:666670.
[18] Varghese S, Das S. Role of molecular packing in determining solid-state optical properties of π-conjugated materials. J Phys Chem Lett 2011;2:863–73.
[19] Yoon SJ, Park SY. Polymorphic and mechanochromic luminescence modulation in the highly emissive dicyanodistyrylbenzene crystal: secondary bonding interaction in molecular stacking assembly. J Mater Chem 2011;21:8338–46.
[20] Wang Y, Liu W, Bu L, Li J, Zheng M, Zhang D, et al. Reversible piezochromic luminescence of 9,10-bis[(N-alkylcarbazol-3-yl)vinyl]anthracenes and the dependence on N-alkyl chain length. J Mater Chem C 2013;1:856–62.
[21] Bu L, Sun M, Zhang D, Liu W, Wang Y, Zheng M, et al. Solid-state fluorescence properties and reversible piezochromic luminescence of aggregation-induced emission-active 9,10-bis[(9,9-dialkylfluorene-2-yl)vinyl]anthracenes. J Mater Chem C 2013;1:2028–35.
[22] Shan GG, Li HB, Sun HZ, Zhu DX, Cao HT, Su ZM. Controllable synthesis of iridium(III)-based aggregation-induced emission and/or piezochromic luminescence phosphors by simply adjusting the substitution on ancillary ligands. J Mater Chem C 2013;1:1440–9.
[23] Zhang X, Chi Z, Zhang J, Li H, Xu B, Li X, et al. Piezofluorochromic properties and mechanism of an aggregation-induced emission enhancement compound containing N-hexyl-phenothiazine and anthracene moieties. J Phys Chem B 2011;115:7606–11.
[24] Luo X, Zhao W, Shi J, Li C, Liu Z, Bo Z, et al. Reversible switching emissions of tetraphenylethene derivatives among multiple colors with solvent vapor, mechanical, and thermal stimuli. J Phys Chem C 2012;116:21967–72.
[25] Zhang X, Chi Z, Zhou X, Liu S, Zhang Y, Xu J. Influence of carbazolyl groups on properties of piezofluorochromic aggregation-enhanced emission compounds containing distyrylanthracene. J Phys Chem C 2012;116:23629–38.
[26] Han T, Zhang YJ, Feng X, Lin ZG, Tong B, Shi JB, et al. Reversible and hydrogen bonding-assisted piezochromic luminescence for solid-state tetraaryl-buta-1,3-diene. Chem Commun 49:7049–51.
[27] Zhang Z, Yao D, Zhou T, Zhang H, Wang Y. Reversible piezo- and photochromic behaviors accompanied by emission color switching of two anthracene-containing organic molecules. Chem Commun 2011;47:7782–4.
[28] Chen F, Zhang J, Wan X. Design and synthesis of piezochromic materials based on push–pull chromophores: a mechanistic perspective. Chem Eur J 2012;18:4558–67.
[29] Lee WE, Lee CL, Sakaguchi T, Fujiki M, Kwak G. Piezochromic fluorescence in liquid crystalline conjugated polymers. Chem Commun 2011;47:3526–8.